Molecular Crystals and Liquid Crystals
Publication details, including instructions for authors and subscription information:
http://www.tandfonline.com/loi/gmcl20

Nematic Bistable Device Using a Metastable Anti-Conical Surface Anchoring

Ivan Dozov [a b], Luc Faget [c] & Ph. Martinot-Lagarde [d]

[a] Laboratoire de Physique des Systèmes Complexes, Université de Picardie Jules Verne, 33 rue Saint Leu, 80039, AMIENS Cedex 1, France

[b] Institute of Solid State Physics, Bulgarian Academy of Sciences, 72 blvd., Tsarigradsko Chaussee, 1784, Sofia, Bulgaria

[c] On leave from Nemoptic, 1 rue Guynemer, F-78114, Magny-les-Hameaux, France

[d] Laboratoire de Physique des Solides, UMR 8502 CNRS—Université Paris-Sud, Bât. 510, 91405, Orsay Cedex, France

Version of record first published: 15 May 2012.

To cite this article: Ivan Dozov , Luc Faget & Ph. Martinot-Lagarde (2012): Nematic Bistable Device Using a Metastable Anti-Conical Surface Anchoring, Molecular Crystals and Liquid Crystals, 560:1, 75-81

To link to this article: http://dx.doi.org/10.1080/15421406.2012.663180

Mol. Cryst. Liq. Cryst., Vol. 560: pp. 75–81, 2012

ISSN: 1542-1406 print/1563-5287 online
DOI: 10.1080/15421406.2012.663180

Taylor & Francis
Taylor & Francis Group

Nematic Bistable Device Using a Metastable Anti-Conical Surface Anchoring

IVAN DOZOV,[1,*] LUC FAGET,[2]
AND PH. MARTINOT-LAGARDE[3]

[1]Laboratoire de Physique des Systèmes Complexes, Université de Picardie Jules Verne, 33 rue Saint Leu, 80039 AMIENS Cedex 1, France; Institute of Solid State Physics, Bulgarian Academy of Sciences, 72 blvd. Tsarigradsko Chaussee, 1784 Sofia, Bulgaria
[2]On leave from Nemoptic, 1 rue Guynemer, F-78114 Magny-les-Hameaux, France
[3]Laboratoire de Physique des Solides, UMR 8502 CNRS—Université Paris-Sud, Bât. 510, 91405 Orsay Cedex, France

We propose a bistable nematic device implementing the recently observed anti-conical degenerated anchoring on a grafted polystyrene surface. The anti-conical surface presents two energy minima, planar degenerated and homeotropic, separated by a conical energy barrier. Under moderate electric field the anchoring is broken, the surface director jumps across the energy barrier and the device switches between two optically distinct bistable textures.

Keywords Anchoring transitions; bistable nematic; surface bistability

1. Introduction

The surface anchoring is one of the most important properties of the nematics for both fundamental research and applications. The interface liquid crystal/substrate has lower symmetry than the bulk nematic and defines some preferred directions $\mathbf{n}_e$, called "easy" axis, for the alignment of the nematic surface director $\mathbf{n}_s$. For common monostable anchorings $\mathbf{n}_e$ is unique and any deviation $\delta\mathbf{n}_s = \mathbf{n}_s - \mathbf{n}_e$ costs an anchoring energy $W(\delta\mathbf{n}_s)$. In a first approximation $W(\delta\mathbf{n}_s)$ contains two independent zenithal (out-of-plane) and azimuthal (in-plane) Rapini-Papoular (RP) terms [1]:

$$W(\theta_s, \varphi_s) = -\frac{1}{2}A_{zen}\cos^2(\theta_s - \theta_e) - \frac{1}{2}A_{az}\cos^2(\varphi_s - \varphi_e)$$

where θ_s, φ_s are the spherical coordinates of $\mathbf{n}_s$ and A_{zen}, A_{az} are the anchoring strength coefficients.

Bistable or multistable anchorings, with several distinct easy axes, have been reported on cleaved crystals [2], evaporated SiO films [3], nano-structured [4,5] polymers and other anisotropic surfaces. Continuously degenerated anchorings, with energy minimized

*Address correspondence to Ivan Dozov, LPSC, Université de Picardie Jules Verne, 33 rue Saint Leu, 80039 AMIENS Cedex 1, France. E-mail: i.dozov@free.fr

on an "easy surface", could also exist, for example on isotropic boundaries. A zenithal degeneration cannot be expected—even for an isotropic substrate, its normal **N** is a particular direction, along which the nematic order varies rapidly. By symmetry, terms like $(\mathbf{n}_s \cdot \mathbf{N})^{2m} = cos(\theta_s)^{2m}$, with m integer, are always allowed and contribute to the zenithal anchoring energy. On the contrary, all the azimuthal directions on isotropic surfaces are equivalent and A_{az} should vanish, as e.g. on the interface nematic/isotropic fluid.

On solid substrates the azimuthal degeneration is often hindered by the anchoring memory [6–8]. However, several kinds of degenerated alignments were reported on memory-free polymer surfaces. In the planar degenerated case [9] the easy directions form an "easy plane", defined by $\theta_s = \pi/2$. For the conical anchoring [10] the energy minima are along an "easy cone", defined by $\theta_s = \theta_c < \pi/2$. The recently reported [11] anti-conical anchoring presents two metastable states, homeotropic and planar degenerated, separated by a conical anchoring "barrier", a maximum of the energy at $\theta_s = \theta_a$, with $0 < \theta_a < \pi/2$.

Here we study the texture transitions under electric field in nematic cells with anti-conical alignment. We observe a surface anchoring breaking, with surface director jumping across the anchoring energy barrier. We demonstrate a simple anti-conical device based on this phenomenon, switching between two optically distinct bistable textures.

2. General form of the Zenithal Energy of the Azimuthally Degenerated Anchoring

The simple RP-approximation is inadequate for the conical and anti-conical degenerated anchorings. Large positive [10] or negative [11] $\cos^4\theta_s$ terms are required respectively to describe these states. The existence of these terms has been theoretically predicted [12] and experimentally observed close to anchoring transitions, driven by the temperature [13,14] or by the alignment layer treatment [15].

For azimuthally degenerated anchorings the energy $W = W(\theta_s)$ is independent on the in-plane orientation φ_s. The symmetry of the surface (rotation around **N**) and of the nematic (inversion of the director **n**) imposes $W(\theta_s) = W(-\theta_s) = W(\pi \pm \theta_s)$. The most general form of $W(\theta_s)$ is then [11]:

$$W(\theta_s) = \frac{1}{2}\alpha \cos(2\theta_s) + \frac{1}{4}\beta \cos(4\theta_s) + \frac{1}{6}\gamma \cos(6\theta_s) + \cdots \tag{1}$$

where α is the RP term and $\beta, \gamma, \ldots$ are higher order contributions. For simplicity we keep here only the first two terms, sufficient to describe the observed degenerated anchorings.

Figure 1 presents the energy functions of the different anchoring states, obtained by minimization of $W(\theta_s)$ (for $\alpha > 0$, as measured in the experiment). For small β coefficient, $|\beta| < \alpha/2$, the anchoring is planar degenerated (curve 1). For large positive β, $\beta > \alpha/2$, the anchoring is conical (curve 2), with energy maxima at $\theta_s = 0$ and $\theta_s = \pi/2$, and a minimum on the easy cone, defined by $\theta_c = \frac{1}{2}\arccos(\alpha/2\beta)$. For large negative β, $\beta < -\alpha/2$, the anchoring is anti-conical (curve 3): $W(\theta_s)$ has two distinct minima, at $\theta_s = 0$ and $\theta_s = \pi/2$, and a maximum on the anchoring barrier, defined by $\theta_a = \frac{1}{2}\arccos(-\alpha/2\beta)$. In general, the two minima have different energies, one of them being only metastable. However, once switched to this minimum, the surface cannot go back spontaneously over the anchoring barrier - we expect then a true bistability of the bulk textures.

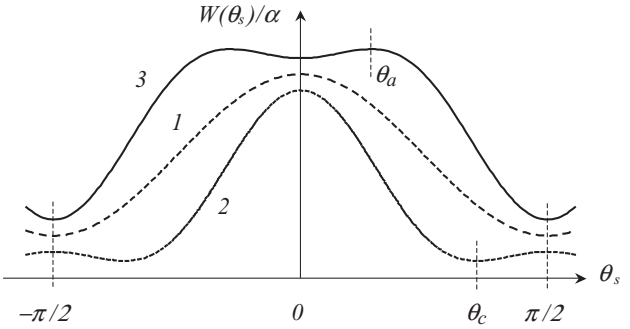

Figure 1. Zenithal anchoring energy for azimuthally degenerated surfaces for $\alpha > 0$ and different α/β values: 1—Planar state ($\alpha/\beta = 0$) , $W(\theta_s)$ presents only two extrema, a minimum at $\theta_s = \pi/2$ and a maximum at $\theta_s = 0$; 2—Conical state ($\alpha/\beta = 0.8$), $W(\theta_s)$ presents two maxima and a minimum at $\theta_s = \theta_c$; 3—Anti-conical state ($\alpha/\beta = -0.8$), the two minima of $W(\theta_s)$ are separated by an anchoring barrier at $\theta_s = \theta_a$.

3. Experimental Study of the Anti-Conical Anchoring

We realize the anti-conical anchoring with the nematic n-heptyl-cyanobyphenyl (7CB) and a grafted polystyrene (PS) alignment layer, reported [11] to give temperature-controlled anchoring transitions between all the three degenerated states shown on Fig. 1. We study the surface switching under field in a thin cell ($d = 1.7$ μm) with ITO electrodes on both plates. One of the plates is PS treated [11], to give anti-conical degeneration below $T = 16.4$°C. The opposite plate has strong monostable planar anchoring (SiO evaporation), removing the azimuthal degeneration of the bulk texture. To avoid polar effects, due to charge accumulation on the surfaces, we apply the field in AC bursts ($f > 10$ kHz), with variable duration and modulated amplitude U. The voltage-dependence of the optical retardation $L(U)$ is measured in real time (time-resolution of about 10 ms, limited by the bulk texture response time) using an electro-optical setup [16–18] and a polarizing microscope. In the same burst, we vary U continuously from zero up to several volts and back to zero, to obtain the two-way electro-optical curve and to detect eventual hysteresis.

The typical $L(U)$ dependence is shown in Fig. 2(a). At $U = 0$ the cell retardation is $L_0 = 350$ nm, compatible with $L_0 = d{\cdot}\Delta n$ expected for a planar texture. The zero pretilt angle on both plates is confirmed by the sharp Fréedericksz [19] threshold at $U_F = 0.96$ V. At $U > U_F$, L decreases rapidly due to the director reorientation in the bulk and on the PS surface. At $U = U_C = 2.57$ V the birefringence changes abruptly, decreasing by $\delta L = 16$ nm, indicating a first-order anchoring breaking [20] on the PS layer. To understand this phenomenon, we plot in Fig. 2(b) the graphic solution of the surface torque balance equation. The anchoring torque $-\Gamma_s = \alpha \sin(2\theta_s)[1 + (2\beta/\alpha)\sin(4\theta_s)]$ is presented by a solid line. The dashed lines show the integrated bulk dielectric torque Γ_{diel} transmitted to the surface. Taking for simplicity $K_{33} = K_{11}$ and $U \gg U_F$ we obtain [20] $\Gamma_{diel} \cong \pi K_{33}$ $sin\theta_s$ $U/(dU_F)$. For $U < U_F$ there are two stable solutions: the stable planar state P and the metastable homeotropic one H. Above U_F, the planar solution shifts to smaller θ_s values, as $\mathbf{n}_s$ tilts under the increasing dielectric torque, while the homeotropic solution remains unchanged. Above $U = U_C$, the anchoring breaking threshold, Γ_s is too weak to equilibrate Γ_{diel} and the surface jumps to $\theta_s = 0$, the unique equilibrium point for $U > U_C$. Decreasing back the field, the surface remains in the local minimum H, due to the anchoring barrier.

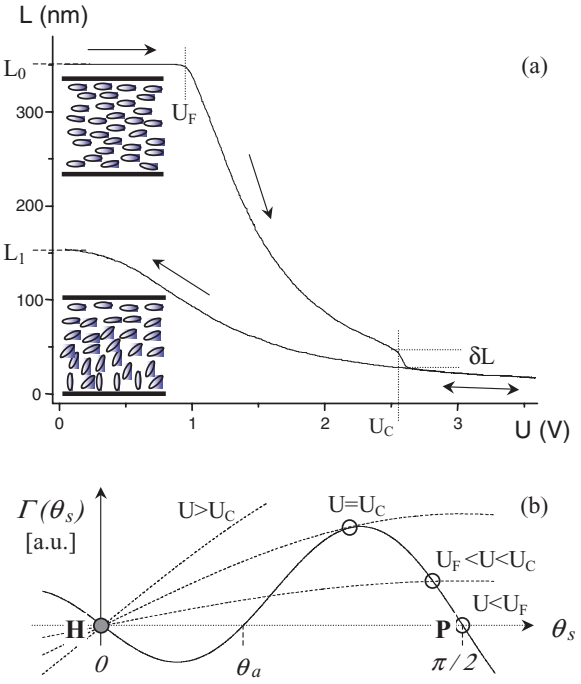

Figure 2. Electro-optical response and anchoring breaking in the anti-conical state at $T = 11.5°$C: (a) Experimentally measured birefringence of the cell. The arrows indicate the evolution of the curve as the voltage increases and then decreases back to zero. The pictures show the initial and the final textures at $U = 0$; (b) Torque equilibrium and anchoring breaking ($\alpha = 0.72$, $\beta = -0.49$). The solid curve represents the anchoring torque, the dashed ones show the dielectric torque transmitted to the surface at increasing field. The circles show the equilibrium solutions before (open) and after (full) the anchoring breaking.

This behavior is clearly seen in Fig. 2(a): when U decreases back to 0, the phase shift saturates to a new value $L_1 \approx L_0/2$, as expected for a hybrid texture (planar on the SiO side and homeotropic on the PS one).

From the values of the threshold U_C and the birefringence jump δL we obtain the anchoring strength coefficients α and β. At $T = 11.5°$C, $\alpha = 0.72$, $\beta = -0.49$, and they vary rapidly with the temperature [11]. The numerical fitting of the electro-optical curve, taking into account $K_{33} \neq K_{11}$ and the finite U_C/U_F ratio, confirms the above approximate results. Throughout the temperature range of the anti-conical state ($16.4°\text{C} > T > 6°\text{C}$) the anchoring breaking threshold $E_C = U_C/d$ is remarkably weak and constant, $E_C = 1.7 \pm 0.2$ V/μm, one order of magnitude lower than reported for other "weak" anchoring [4,21–24] surfaces.

4. Bistable Anti-Conical Device

The observed bistability and weak threshold are promising for applications. Bistable devices switching between two distinct surface states, i.e. with surface bistability, have been proposed before [4,23,24]. However, these bistable surfaces are difficult to realize, needing a surface topography or modulation of the anchoring properties on a sub-micrometer scale.

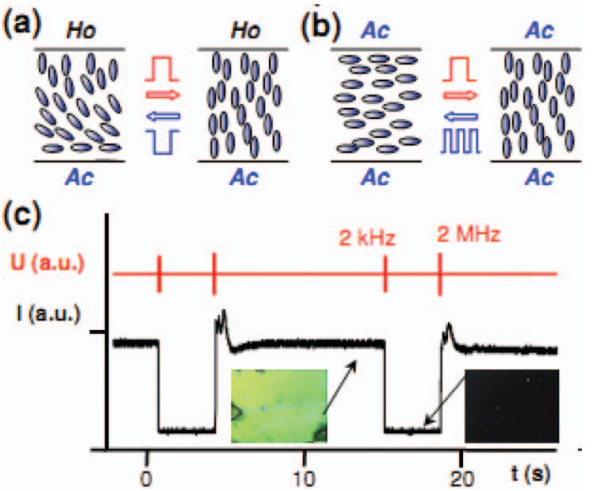

Figure 3. Examples of anti-conical bistable devices: (a) With only one anti-conical (*Ac*) surface and polar driving; (b) With two anti-conical surfaces and dual-frequency driving scheme; (c) Optical response of the device on Fig. 3(a), driven with dual-frequency AC bursts. The photographs show the two bistable states under crossed linear polarizers.

In contrast, the anti-conical bistable anchoring is realized on uniform isotropic substrates, without nano-structuring, by a cheap and reliable self-assembly-like grafting process. The bistable states, homeotropic and planar, are optically the most distinct possible, resulting in a good contrast. The high energy barrier between them provides a long term bistability, but the switching threshold remains weak, about *2* V/μm.

One possible architecture of anti-conical bistable device is presented on Fig. 3(a). The cell has one anti-conical surface (*Ac*) and opposite homeotropic (*Ho*) alignment. The two bulk bistable textures are respectively hybrid and homeotropic. Fast switching from hybrid to homeotropic is obtained by anchoring breaking. For the switching back to the planar state, one can use in this geometry a polar coupling with the electric field. In fact, the flexoelectric polarization [25], bulk or surface-like, has been already proposed for polar control of monostable [26,27] or bistable nematic devices [4,21–24]. Experimentally, under short DC pulses we observe a strong polar electro-optical response of the cell, one order of magnitude stronger than the expected [28,29] flexoelectric one. This effect is probably due to a surface polarization [30,31], e.g. of ordoelectric origin [32], and might be used for reversible switching between the two bistable states, controlled by a short "selection" DC pulse after the anchoring breaking.

The optimal optical configuration of the device is under crossed *circular* polarizers, to avoid artifacts due to the azimuthally degenerated hybrid state. The homeotropic texture gives an excellent black state for any cell thickness d, while the hybrid state is bright when its optical thickness $\sim d\Delta n/2$ is close to $\lambda/2$ ($d \cong 3$ μm for $\Delta n \cong 0.2$, a good compromise ensuring easy fabrication and fast relaxation).

Another configuration of the bistable anti-conical device (Fig. 3(b)) uses anti-conical anchoring on both surfaces. The bistable textures in this case, homeotropic and degenerated planar, are optically the most distinct possible. The optimal thickness is now $d \cong \lambda/(2\Delta n)$, typically $d < 2$ μm, and fast relaxation times are expected. A field-controlled switching back to the planar state might be obtained by using a nematic with frequency-dependent

sign of $\Delta\varepsilon$ and dual-frequency driving [33,34]. In fact, varying the frequency, the sign of the torque applied on the anti-conical surface is inversed, enabling an anchoring breaking toward any one of the two bistable textures. However, for the practical implementation of this driving scheme we need dual-frequency nematic material presenting anti-conical anchoring, still to be developed.

In Fig. 3(c) we show the optical response of the hybrid device of Fig. 3(a) (nematic 7CB on grafted PS layer, $T = 11.5°C$, $d \cong 9\ \mu$m). The cell is driven with dual-frequency AC bursts ($U \cong 20$ V, pulse duration 10–100 ms). Starting from the planar state, we apply a low frequency (2 kHz) field, strong enough to break the anti-conical anchoring. The cell switches into the metastable homeotropic state and remains there after the end of the driving pulse, trapped in the local minimum of the total energy. Applying then a high frequency (2 MHz) pulse, we observe that the cell switches back to the initial planar state. This switching back is not obtained by an anchoring breaking, but by the nucleation of a dense network of defects on the PS surface. This allows the relaxation of the metastable homeotropic state to the planar one by defects propagation, instead of the forbidden uniform transition through the energy barrier. In both ways the switching of the surface is fast (<1 ms). The bulk relaxation to the planar state, however, is much slower, due to the large cell thickness and the high viscosity of 7CB at $T = 11.5\,°C$. Despite the higher total energy of the homeotropic texture, the device shows infinite bistability—the anchoring barrier between the two states is high enough to prevent spontaneous transition to the hybrid texture.

5. Summary

We propose bistable applications of the recently reported anti-conical anchoring. We study electro-optically the switching of the anti-conical surface by a low threshold anchoring breaking. We propose bistable devices using the anti-conical anchoring, confirming experimentally the expected switching and bistability. Further development of the anti-conical alignment layers and nematic materials is still needed for the practical realization of a new generation of bistable displays and/or optical valves with fast surface switching. However, other groups recently reported [35–37] similar metastable coexistence of homeotropic and planar anchoring states in a number of other nematic/alignment layer systems, indicating that the anti-conical anchoring behavior is not so rare and unique.

Acknowledgments

We are grateful to Dr. S. Joly and Dr. D.-N. Stoenescu for helpful discussions. The work by L.F. was supported by a CIFRE grant from ANRT, France.

References

[1] Rapini, A., & Papoular, M. (1969). *J. Phys. (Paris) Coll.C4*, *30*, 54.
[2] Bechhoefer, J., Jerome, B., & Pieranski, P. (1990). *Phys. Rev. A*, *41*, 3187.
[3] Monkade, M., Boix, M., & Durand, G. (1988). *Europhys. Lett.*, *5*, 697.
[4] Bryan-Brown, G. P., Brown, C. V., Sage, I. C., & Hui, V. C. (1998). *Nature*, *392*, 365.
[5] Kim, J. H., Yoneya, M., & Yokoyama, H. (2002). *Nature*, *420*, 159.
[6] Cheng, J., & Boyd, G. D. (1979). *Appl. Phys. Lett.*, *35*, 444.
[7] Jerome, B. (1991). *Reports on Progress in Physics*, *54*, 391.
[8] Barberi, R., *et al.* (1998). *Liq. Cryst.*, *25*, 23.
[9] Dozov, I., *et al.* (2000). *Appl. Phys. Lett.*, *77*, 4124.
[10] Ou Ramdane, O., *et al.* (2000). *Phys. Rev. Lett.*, *84*, 3871.

[11] Faget, L., *et al.* (2006). *Phys. Rev. E*, *74*, 050701.
[12] Fournier, J. B., & Galatola, P. (2005). *Europhys. Lett.*, *72*, 403.
[13] Nobili, M., & Durand, G. (1992). *Phys. Rev. A*, *46*, R6174.
[14] Nobili, M., & Durand, G. (1994). *Europhys. Lett.*, *25*, 527.
[15] Carbone, G., & Rosenblatt, C. (2005). *Phys. Rev. Lett.*, *94*, 057802.
[16] Lamarque-Forget, S., Martinot-Lagarde, P., & Dozov, I. (2001). *Jpn. J. Appl. Phys. Part 2 - Lett.*, *40*, L349.
[17] Lamarque-Forget, S., et al. (2000). *Adv. Mater.*, *12*, 1267.
[18] Martinot-Lagarde, P., Dreyfus-Lambez, H., & Dozov, I. (2003). *Phys. Rev. E*, *67*, 051710.
[19] Freedericksz, V., & Zolina, V. (1933). *Transactions of the Faraday Society*, *29*, 919.
[20] Dozov, I., & Martinot-Lagarde, P. (1998). *Phys. Rev. E*, *58*, 7442.
[21] Dozov, I., Nobili, M., & Durand, G. (1997). *Appl. Phys. Lett.*, *70*, 1179.
[22] Bryan-Brown, G. P., Wood, E. L., & Sage, I. C. (1999). *Nature*, *399*, 338.
[23] Barberi, R., Giocondo, M., Lagarde, P. M., & Durand, G. (1993). *Appl. Phys. Lett.*, *62*, 3270.
[24] Barberi, R., et al. (1997). *Appl. Phys. Lett.*, *71*, 3495.
[25] Meyer, R. B. (1969). *Phys. Rev. Lett.*, *22*, 918.
[26] Dozov, I., Martinot-Lagarde, P., & Durand, G. (1982). *Journal de Physique Lettres*, *43*, L365.
[27] Rudquist, P., Komitov, L., & Lagerwall, S. T. (1994). *Phys. Rev. E*, *50*, 4735.
[28] Dozov, I., Martinot-Lagarde, P., & Durand, G. (1983). *Journal de Physique Lettres*, *44*, L817.
[29] Dozov, I., Penchev, I., Martinot-Lagarde, P., & Durand, G. (1984). *Ferroelectr. Lett. Sect.*, *2*, 135.
[30] Lavrentovich, O. D., et al. (1991). *Zh. Eksp. Teor. Fiz.*, *99*, 777.
[31] Komitov, L., Helgee, B., Felix, J., & Matharu, A. (2005). *Appl. Phys. Lett.*, *86*, 023502.
[32] Barbero, G., Dozov, I., Palierne, J. F., & Durand, G. (1986). *Phys. Rev. Lett.*, *56*, 2056.
[33] Bucher, H. K., Klingbie, R. T., & VanMeter, J. P. (1974). *Appl. Phys. Lett.*, *25*, 186.
[34] Stein, C. R., & Kashnow, R. A. (1971). *Appl. Phys. Lett.*, *19*, 343.
[35] Dhara, S., *et al.* (2009). *Phys. Rev. E*, *79*, 060701.
[36] Lee, G., *et al.* (2010). *Liq. Cryst.*, *37*, 883.
[37] Nazarenko, V. G., *et al.* (2010). *Phys. Rev. Lett.*, *105*, 017801.